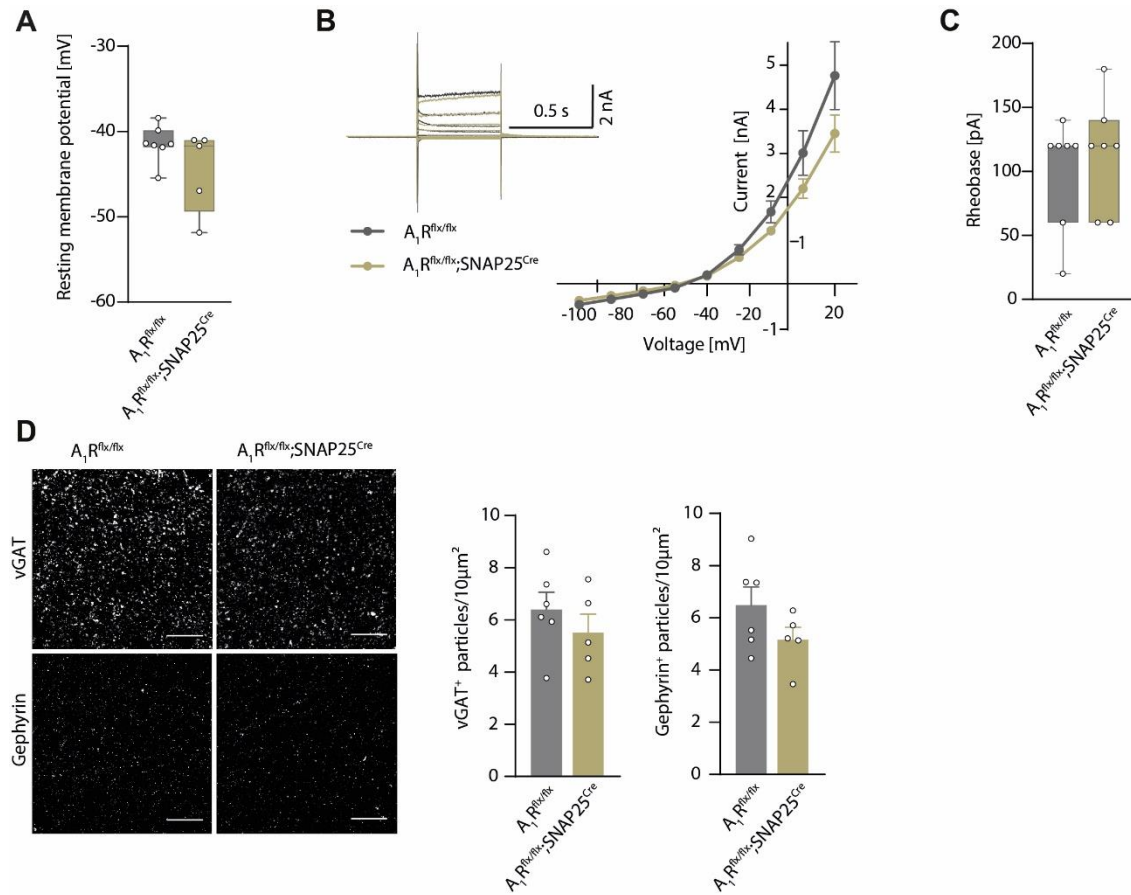


## Supplementary Figure 2



**Supplementary Figure 2 | No apparent differences in membrane properties between  $A_1R$ -proficient and  $A_1R$ -deficient mitral cells.** (A) Current-clamp recording of resting membrane potential of mitral cells in acute slices of  $A_1R^{flx/flx}$  and  $A_1R^{flx/flx};SNAP25^{Cre}$  animals. Measurement was performed immediately after establishing whole cell configuration,  $BF_{10} = 0.929$ . (B) Current-voltage relationship recorded in voltage clamp (from  $-100$  to  $20$  mV in  $15$  mV steps, see inset) in whole cell conductance in mitral cells of both genotypes ( $BF_{10} = 0.514-0.998$  for different voltage steps). (C) Firing behavior was analyzed by application of depolarizing current injections of consecutively higher amplitude. Rheobase shows the first current step resulting in a membrane depolarization beyond the action potential threshold in  $A_1R^{flx/flx}$  ( $91 \pm 17$  pA,  $n = 7$  slices of 5 mice) and  $A_1R^{flx/flx};SNAP25^{Cre}$  ( $112 \pm 23$  pA,  $n = 5$  slices of 4 mice) ( $BF_{10} = 0.559$ ). In A–C only cells with phenotypically confirmed  $A_1R$  function or absence, respectively, as detected by application of adenosine during the later course of recording were considered. Displayed voltage is not corrected for liquid junction potential. Boxplots show mean to max values. (D) Representative images and quantification of inhibitory synaptic density in the external plexiform layer (EPL) of the main olfactory bulb in  $A_1R$ -proficient ( $A_1R^{flx/flx}$ ) and  $A_1R$ -deficient ( $A_1R^{flx/flx};SNAP25^{Cre}$ ) mice. Immunohistochemical stainings comprised the presynaptic protein vGAT ( $BF_{10} = 0.622$ ) and the postsynaptic protein gephyrin ( $BF_{10} = 0.917$ ) in the EPL in  $A_1R^{flx/flx}$  ( $n = 6$ ) and  $A_1R^{flx/flx};SNAP25^{Cre}$  ( $n = 5$ ) (Scale bar =  $20 \mu m$ ).